

DOI: 10.1039/C4DT02706J

## Speciation and structure of tin(II) in hyper-alkaline aqueous solution

Eva G. Bajnóczi,<sup>a,h</sup> Eszter Czeglédi,<sup>a,h</sup> Ernő Kuzmann,<sup>b</sup> Zoltán Homonnay,<sup>b</sup> Szabolcs Bálint,<sup>c</sup> György Dombi,<sup>d</sup>  
Péter Forgo,<sup>d</sup> Ottó Berkesi,<sup>e</sup> István Pálinkó,<sup>f,h</sup> Gábor Peintler,<sup>e,h</sup> Pál Sipos,<sup>a,h\*</sup> and Ingmar Persson<sup>g\*</sup>

### 5 Abstract

The structure of tin(II) hydroxido complex forming in hyper-alkaline aqueous solutions ( $0.2 \leq C_{\text{NaOH}} \leq 12 \text{ mol}\cdot\text{dm}^{-3}$ ) has been determined by EXAFS, Raman and Mössbauer spectroscopy, and the general composition by potentiometric titrations. Experimental work was supplemented by computational means. The mean Sn-O distance in the non-linear complex is remarkably short, 2.078 Å. From single crystal X-ray data of O-coordinated Sn(II) compounds, for the given coordination numbers of  $N = 2$  and 3, the bond distances were found to cover a relatively wide range (much wider than normal). The experimentally determined Sn-O bond distance is within the range of both. Thermodynamic studies using  $\text{H}_2/\text{Pt}$  electrode up to free hydroxide concentrations of  $1 \text{ mol}\cdot\text{dm}^{-3}$  have shown the presence of a single complex with a tin(II):hydroxide ratio of 1:3. These findings together with Raman and Mössbauer spectroscopic measurements supplemented by quantum mechanical calculations proved that the predominating complex is  $[\text{Sn}(\text{OH})_3]^-$  and that the presence of  $[\text{SnO}(\text{OH})]^-$  cannot be experimentally proven. It is also shown that at pH values above 13 the structure of the predominating trihydroxidotin(II) complex is not affected by the presence of high concentrations of chloride ions.

### Introduction

Under hyperalkaline conditions ( $\text{pH} > 13$ ) in aqueous systems, inorganic cations are capable of forming solution species (both mono- and polynuclear)<sup>1,2</sup> which are not detectable in solutions with medium pH-s. Crystallization from such solutions often yields solid materials with peculiar local- and nanostructure.<sup>3,4</sup> Knowledge of the structure and dynamics of the solution species forming under these extreme conditions could be the key to understand and to manipulate a range of aquatic processes (from industrial to geochemical ones).

Hydrolysis of metal ions (the structure, composition and thermodynamics of their hydroxido complexes) is one of the classical topics of inorganic solution chemistry: formation constants for a large variety of hydroxido complexes as well as solubility products of solid metal hydroxides are well known and are collated in various textbooks and tables.<sup>5,6</sup> Traditionally, species forming in solutions with  $2 < \text{pH} < 12$  are mostly characterized, and the knowledge on the nature of hydroxido complexes at the extremely alkaline end of the pH scale are generally unknown. This is due to well-known theoretical as well as practical/technical difficulties. In spite of these hurdles, the

number of publications dealing with this particular aspect of solution chemistry steadily increases. For obvious reasons, metal ions with reasonable solubility (*e.g.*, amphoteric ones) are most intensely studied (*e.g.*,  $\text{Al}(\text{III})$ <sup>7-9</sup>,  $\text{Ga}(\text{III})$ <sup>10,11</sup>,  $\text{Cr}(\text{III})$ <sup>12,13</sup>,  $\text{Pb}(\text{II})$ <sup>14</sup>,  $\text{Tl}(\text{I})$ <sup>15,16</sup>, *etc.*). Beside these, data for metal ions that are hardly soluble in alkaline conditions also emerge (*e.g.*,  $\text{Cu}(\text{II})$ <sup>17</sup>,  $\text{Fe}(\text{III})$ <sup>18</sup>, actinides<sup>19</sup>, *etc.*)

In the current paper, we will focus on the behaviour of the amphoteric Sn(II) ion in hyperalkaline media. Several aqueous species of Sn(II) are known from the literature. Stannous ion forms the stepwise hydroxido complexes with formal compositions of  $[\text{Sn}(\text{OH})]^+$ ,  $[\text{Sn}(\text{OH})_2]^0$  and  $[\text{Sn}(\text{OH})_3]^-$  at low metal concentrations, while in solutions with higher Sn(II) concentrations, polynuclear  $[\text{Sn}_2(\text{OH})_2]^{2+}$  and  $[\text{Sn}_3(\text{OH})_4]^{2+}$  species have also been observed.<sup>20-22</sup> On the basis of the literature data<sup>1,2,20-22</sup>, in the last stepwise hydroxido complex of the stannous ion, the  $\text{OH}^-:\text{Sn}(\text{II})$  ratio is 3:1. No higher complexes could have been extracted from potentiometric measurements up to equilibrium  $\text{OH}^-$  concentrations of 0.25 M.<sup>23</sup> However, under strongly alkaline conditions the formation of  $[\text{Sn}(\text{OH})_4]^{2-}$  or even  $[\text{Sn}(\text{OH})_6]^{4-}$  was claimed to be possible.<sup>24</sup>

The main objective of the present work is to reveal the identity and structure of the tin(II) complex(es) present in aqueous solution at  $\text{pH} > 13$ . Systematic X-ray absorption spectroscopy (XAS), Raman and Mössbauer spectroscopic measurements on solutions containing NaOH ( $0.1 \leq C_{\text{NaOH}} \leq 16 \text{ mol}\cdot\text{dm}^{-3}$ ) and tin(II) ( $0.05 - 0.25 \text{ mol}\cdot\text{dm}^{-3}$ ) and pH potentiometric titrations have been carried out. From a practical point of view it is also important to clarify whether or not chloride as counter ion has any effect on the local environment of tin(II) at high hydroxide concentrations.

### Experimental section

#### 80 Reagents and solutions

Analytical grade NaOH (ANALR NORMAPUR) or KOH (Reanal) was dissolved in distilled water with intensive stirring and cooling to prepare the alkaline stock solution. The concentration was calculated from the density of the solution, determined by a picnometer, according to literature procedures.<sup>25</sup> The carbonate content was minimized as described elsewhere.<sup>26</sup> The stock solution was stored in a caustic resistant Pyrex bottle with a tightly fitted screw-top.

The tin(II) containing stock solution was prepared in two ways. For the stock solution with  $C_{\text{Sn(II)}} \approx 0.5 \text{ mol}\cdot\text{dm}^{-3}$  and  $C_{\text{acid}} \approx 1 \text{ mol}\cdot\text{dm}^{-3}$ , tin(II) oxide powder, SnO (Sigma Aldrich),

was dissolved was prepared in oxygen-free atmosphere in dilute analytical grade hydrochloric or perchloric acid (Sigma Aldrich). The purity of SnO was checked with powder X-ray diffraction and was found to contain less than *ca.* 2% SnO<sub>2</sub>.

The tin(II) stock solution for the potentiometric titrations,  $C_{\text{Sn(II)}} \approx 0.6 \text{ mol}\cdot\text{dm}^{-3}$  and  $C_{\text{HCl}} \approx 1.5 \text{ mol}\cdot\text{dm}^{-3}$ , was also prepared oxygen free by dissolving metallic tin (Reanal) in diluted analytical grade hydrochloric acid. This process took about four days and during this time the temperature was kept at 50 °C under reflux. A practically tin(IV) free solution could be prepared in this way as the continuously evolving hydrogen gas did secure reducing conditions and any further oxidation of the tin(II) formed was not possible. The solution was filtered under nitrogen atmosphere. The exact concentration of tin(II) was determined by the standard iodometric procedure, while the exact concentration of the hydrochloric acid was determined *via* pH-potentiometric titration with sodium hydroxide.

The alkaline tin(II) solutions for the XAS, Raman and <sup>119</sup>Sn Mössbauer spectroscopy measurements were prepared in a small Pyrex bottle. A custom-made screw-top was fabricated with two small holes for the argon gas in- and outlet and a bigger one for the addition of the tin(II) stock solution. The calculated amount of the freshly prepared tin(II) stock solution was added drop-wise to 25 mL of the appropriately diluted NaOH solution with continuous and intense argon bubbling through the sample and stirring. The NaOH solutions were diluted by weight from the concentrated stock solution, and argon gas was bubbled through it for at least 15 minutes before adding the metal stock solution.

### Potentiometric titrations

The pH potentiometric titrations were carried out using a Metrohm 888 Titrand instrument equipped with H<sub>2</sub>/Pt electrode. The experimental protocol used for such measurements have been described in previous publications.<sup>27,28</sup> The full electrochemical cell contained a platinized hydrogen electrode and a thermodynamic Ag|AgCl reference electrode.

$\text{H}^+/\text{H}_2(\text{Pt}) \mid \text{test sol.}, I = 4 \text{ mol}\cdot\text{dm}^{-3} (\text{NaCl}) \parallel 4 \text{ mol}\cdot\text{dm}^{-3} \text{NaCl} \parallel 4 \text{ mol}\cdot\text{dm}^{-3} \text{NaCl}, \text{Ag}/\text{AgCl}$

The behavior of the electrode was checked and was found to be Nernstian (slope:  $59.2 \pm 0.2 \text{ mV/decade}$ ). The electrode performance was regularly checked *via* calibrations using strong acid- strong base titrations in the concentration range employed during the measurements. All the titrations were performed in an externally thermostated home-made cell and the temperature was kept at  $25.00 \pm 0.04 \text{ }^\circ\text{C}$  by circulating water from a Julabo 12 thermostat. The ionic strength was kept constant,  $I = 4 \text{ mol}\cdot\text{dm}^{-3}$ , with analytical grade NaCl (Prolabo).

### X-ray absorption measurements

The X-ray absorption spectra for tin were collected at the bending magnet beam-line Samba at the Soleil synchrotron facility, Paris, France, which operated at 2.75 GeV and a maximum current of 400 mA. The Samba beam-line covers the energy range 4–42 keV. The maximal flux on the sample at 10 keV is  $1 \times 10^{12} \text{ photon/s/0.1 \% bandwidth}$ . The energy scale of the X-ray absorption spectra were calibrated by assigning the first inflection point of the tin K edges of metallic tin foil to 29200.0 eV.<sup>29</sup> For

recording the spectrum of the tin(II) containing solutions, 15 mL sample was placed in a cubic polyethylene sample holder with a tightly fitted screw-top. The analysis of the data was performed with the EXAFSPAK<sup>30</sup> and FEFF<sup>31</sup> program packages allowing the determination of the structure parameters of the local coordination around tin(II).

### FT-Raman spectroscopy

Raman spectra were recorded on a BIO-RAD Digilab Division dedicated FT-Raman spectrometer equipped with liquid nitrogen cooled germanium detector and CaF<sub>2</sub> beamsplitter. The excitation line was provided by a Spectra Physics T10-106C Nd:YVO<sub>4</sub> laser at 1064 nm. The spectra were recorded between 3600 – 100 cm<sup>-1</sup> with 4 cm<sup>-1</sup> resolution. 4096 scans were collected for each spectrum. The excitation power was 280 mW at the sample position. The spectrometer was controlled by using BIO-RAD Win IR 3.3 software. The samples were placed in a 1 cm pathlength quartz cuvette. Spectra were recorded at room-temperature. Data were processed by the SpekWin software, the fitting of the Lorentzian curves were performed with QtiPlot. (We note here, that attempts were made to collect FT-IR spectra for these solutions in ATR mode. Unfortunately, these were unsuccessful, most probably due to insufficient signal-to-noise ratio.)

### Mössbauer spectroscopy

<sup>119</sup>Sn Mössbauer spectra of frozen solution of the compounds were recorded with a conventional Mössbauer spectrometer (Wissel 5) in transmission geometry with constant acceleration mode at 78 K in a He-cryostat cooled by liquid nitrogen. The measurements were carried out in He atmosphere using a <sup>85</sup>Ba<sup>119m</sup>SnO<sub>3</sub> radiation source of 8 mCi activity. 20 μm α-Fe was used for velocity calibration when a <sup>57</sup>Co/Rh source supplied the γ-rays, and also the isomer shifts are given relative to it. All sample preparations, including also the rapid freezing, were done in a home-made glove-box to minimize the oxidation of the sample. The Mössbauer spectra were analysed by least-square fitting of the Lorentzian lines with the help of the MOSSWINN program.<sup>32</sup> The database of the Mössbauer Effect Data Index was used to interpret the results.

### Computational methods

The complexes studied by computational methods included [Sn(OH)<sub>3</sub>]<sup>-</sup> and [SnO(OH)]<sup>-</sup>, and for comparison, [Sn(H<sub>2</sub>O)<sub>3</sub>]<sup>2+</sup> Sn(OH)<sub>2</sub> [SnO(OH)<sub>2</sub>]<sup>2-</sup>. Optimizations and frequency analyses were performed using the GAUSSIAN 09 program with density functional theory (DFT) at the M052x/6-311++G\*\* computational level. We systematically modeled solvent effects by representing H<sub>2</sub>O as a polarizable continuum, according to the method implemented in the PCM-SCRF (self-consistent reaction field) procedure in the Gaussian program. We take into account some cases explicitly the hydration shell of these complexes, but the calculated properties do not change significantly compared to the PCM method, so we do not discuss those results.

## Results and discussion

The selection of an appropriate, non-interfering counter anion was the first step during the investigation. It is convenient to prepare tin(II) stock solutions using hydrochloric acid as the dissolution is rapid and the solubility of  $\text{SnCl}_2$  is quite high in hydrochloric acid due to the formation of chlorido complexes. The solubility of  $\text{Sn}(\text{ClO}_4)_2$  is significantly lower than that of  $\text{SnCl}_2$ , and the dissolution of  $\text{SnO}$  or metallic tin is much slower in perchloric than in hydrochloric acid. It is therefore important to secure that tin(II)-chlorido complexes are not out-competing the tin(II)-hydroxido complexes in strong alkaline solution. As no literature data are available for the tin(II)-chloride system at  $\text{pH} > 13$ , X-ray absorption spectroscopy was applied to study if tin(II)-chlorido or chlorido-hydroxido mixed complexes are formed under such conditions or not. XAS spectra of  $0.1 \text{ mol}\cdot\text{dm}^{-3}$   $\text{SnCl}_2$  in  $1 \text{ mol}\cdot\text{dm}^{-3}$  hydrochloric acid, in  $4 \text{ mol}\cdot\text{dm}^{-3}$  NaOH, and in  $4 \text{ mol}\cdot\text{dm}^{-3}$  NaOH +  $1 \text{ mol}\cdot\text{dm}^{-3}$  NaCl, were compared with the spectra of  $0.1 \text{ mol}\cdot\text{dm}^{-3}$   $\text{Sn}(\text{ClO}_4)_2$  in  $1 \text{ mol}\cdot\text{dm}^{-3}$  perchloric acid and in  $4 \text{ mol}\cdot\text{dm}^{-3}$  NaOH. The X-ray absorption near-edge structure (XANES) regions and the Fourier-transform of the  $k^3$ -weighted extended X-ray absorption fine structure (EXAFS) data of the measured samples are presented on Figure 1. As the figure shows, the spectra of the two acidic samples are clearly distinguishable by both the near-edge region and the Fourier transform of the EXAFS region.

In  $1 \text{ mol}\cdot\text{dm}^{-3}$  hydrochloric acid tin(II) is almost exclusively present as  $[\text{SnCl}_3]^-$  complex,<sup>33</sup> and the fitting of the spectrum gave a mean Sn-Cl bond distance of  $2.475 \text{ \AA}$ , a Debye-Waller factor ( $\sigma^2$ ) of  $0.0099 \text{ \AA}^2$ , and a coordination number ( $N$ ) of 3, with an assumed trigonal pyramidal geometry, which is in good agreement with the relevant solid crystal structures, (see Table S1). In  $1 \text{ mol}\cdot\text{dm}^{-3}$  perchloric acid tin(II) is present as  $[\text{Sn}(\text{H}_2\text{O})_3]^{2+}$ ,<sup>2</sup> where  $N = 3$ ,  $r = 2.178 \text{ \AA}$ ,  $\sigma^2 = 0.0153 \text{ \AA}^2$ . The EXAFS and Fourier transform fit is shown in Figure S1. On the contrary, the spectra of the three alkaline samples are identical, even if a large excess of chloride ions (1 M) is present. From this, it is clear, that the presence of chloride ions, also in high concentrations, has no effect on the local structure of hydroxidotin(II) complex(es) at these high hydroxide concentrations. Therefore chloride can be considered as truly non-interfering counter ion in the experiments performed in hyper-alkaline aqueous solutions.

In order to establish the composition of the predominating tin(II) complex in hyper-alkaline aqueous solutions, we attempted to determine the tin(II): $\text{OH}^-$  stoichiometric ratio in the complex from potentiometric titrations using an  $\text{H}_2/\text{Pt}$  electrode (suitable to work in hyper-alkaline solutions<sup>27,28</sup>). The total concentrations in the titrated solution were  $0.1998$  and  $1.4992 \text{ mol}\cdot\text{dm}^{-3}$  for tin(II) and NaOH, respectively. The ionic strength was adjusted to  $4.0 \text{ mol}\cdot\text{dm}^{-3}$  with NaCl.

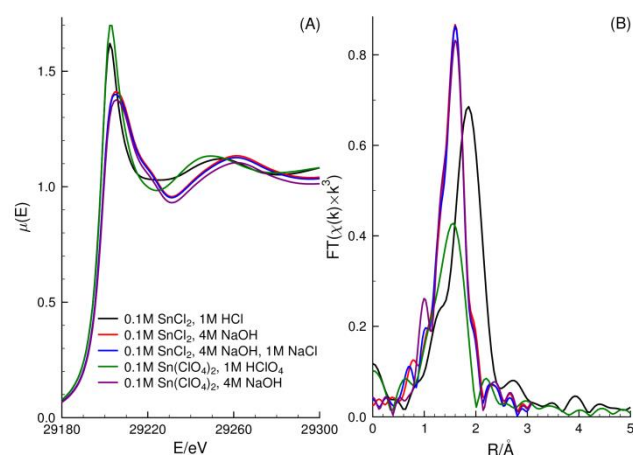


**Fig. 1.** The near-edge region of the Sn K-edge X-ray absorption spectra of  $0.1 \text{ mol}\cdot\text{dm}^{-3}$   $\text{SnCl}_2$  in  $1 \text{ mol}\cdot\text{dm}^{-3}$  hydrochloric acid, in  $4 \text{ mol}\cdot\text{dm}^{-3}$  NaOH, and in  $4 \text{ mol}\cdot\text{dm}^{-3}$  NaOH +  $1 \text{ mol}\cdot\text{dm}^{-3}$  NaCl, compared to the spectra of  $0.1 \text{ mol}\cdot\text{dm}^{-3}$   $\text{Sn}(\text{ClO}_4)_2$  in  $1 \text{ mol}\cdot\text{dm}^{-3}$  perchloric acid and in  $4 \text{ mol}\cdot\text{dm}^{-3}$  NaOH (A) and the Fourier-transform of the  $k^3$ -weighted EXAFS data of them (B)

The titrand was  $3.0825 \text{ mol}\cdot\text{dm}^{-3}$  hydrochloric acid and its ionic strength was also  $4 \text{ mol}\cdot\text{dm}^{-3}$  adjusted with NaCl. A typical titration curve is shown on Figure 2. The system was inhomogeneous from  $7.60 \text{ ml}$  to  $20.80 \text{ ml}$  of the added hydrochloric acid solution (grey area on Figure 2). The inhomogeneity is caused by the precipitation of  $\text{Sn}(\text{OH})_2$  and/or  $\text{SnO}$  since they have very low solubility in the lack of the excess hydroxide. The first equivalence point is close to that point of titration in which the tin(II): $\text{OH}^-$  ratio is 0.5 while the second one corresponds to the complete neutralization of the excess hydroxide. Because of the inhomogeneity, only the initial part of the titration curve (corresponding to titrant consumption  $< 7.60 \text{ mL}$ ) can be evaluated. In this range, only the excess NaOH, unreacted with tin(II) is neutralized by the added hydrochloric acid. Consequently, the change of the observed cell potential ( $E$ ) depends on the concentration of the free hydroxide which is determined by the composition of the  $[\text{Sn}(\text{OH})_x]^{2-x}$  complex.

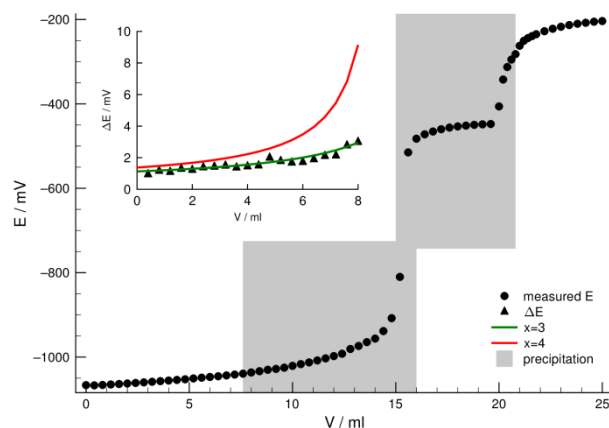


**Fig. 2.** The potentiometric titration curve of  $40 \text{ ml}$  solution containing  $0.1998 \text{ M}$  Sn(II) and  $1.4992 \text{ M}$  NaOH; titrant:  $3.0825 \text{ M}$  HCl. The grey area shows the inhomogeneous region of the titration. Insert: the observed and calculated potential differences for  $x = 3$  and  $4$ , where  $x$  stands for  $[\text{Sn}(\text{OH})_x]^{2-x}$ .

The potential differences between the neighboring titration points,  $\Delta E$ , were used for the evaluation, because the use  $E_0$  (and therefore the experimental uncertainty caused by its inclusion in the evaluation) can be eliminated this way. The theoretical  $\Delta E$  values were calculated from the Nernst-equation assuming  $x = 3$  and 4, exclusively. As it is clearly seen on Figure 2, the calculated  $\Delta E$  values almost perfectly describe the observed ones for  $x = 3$ , indicating that the Sn:OH<sup>-</sup> stoichiometric ratio is strictly (or at least predominantly) 1:3 even at such high hydroxide concentrations. So the formation of [Sn(OH)<sub>4</sub>]<sup>2-</sup> or its

various dehydrated forms ([SnO<sub>2</sub>]<sup>2-</sup> or [SnO(OH)<sub>2</sub>]<sup>2-</sup>) in significant concentrations can be excluded. On the other hand, the formation of [SnO(OH)]<sup>-</sup> (dehydrated form of [Sn(OH)<sub>3</sub>]<sup>-</sup>) might be considered.

The compositions of the alkaline tin(II) solutions prepared for the detailed study of the local structure are shown in Table 1.

The X-ray absorption near-edge structure (XANES) regions of the XAS spectra of them are identical (Figure 3 (A)).

**Table 1** Composition of hyper-alkaline aqueous tin(II) samples studied, expressed in total molar concentrations, and the structure parameters in the refinements of the EXAFS data collected at ambient temperature using the EXAFSPAK program package, including number of Sn-O bond distances,  $N$ , mean Sn-O bond distance,  $d/\text{\AA}$ , and Debye-Waller factor coefficient,  $\sigma^2/\text{\AA}^2$ , the threshold energy,  $E_0/\text{eV}$ , the amplitude reduction factor the goodness,  $S_0^2$ , the goodness of fit,  $F/\%$ , as expressed in the EXAFSPAK program package, ref. 30.

$N=3$	Sn10_2	Sn10_4	Sn10_8	Sn10_12	Sn5_4	Sn15_4	Sn20_4
$C_{\text{NaOH}}$	2	4	8	12	4	4	4
$C_{\text{Sn(II)}}$	0.1	0.1	0.1	0.1	0.05	0.15	0.20
$R$	2.080	2.080	2.075	2.077	2.076	2.078	2.076
$\sigma^2$	0.0040	0.0037	0.0038	0.0039	0.0038	0.0038	0.0040
$E_0$	29225.9	29225.3	29225.6	29226.3	29225.7	29225.7	29225.1
$S_0^2$	1.21	1.21	1.18	1.16	1.18	1.16	1.20
$F$	15.6	13.4	18.0	18.0	14.2	14.6	19.9

The edge positions show that these samples contained exclusively tin(II), as the experimentally observed reference edge energy for tin(II) in solid SnO and for tin(IV) in solid SnO<sub>2</sub> was 29207.45 and 29211.45 eV, respectively, and the edge energy of the samples was found to be 29207.13 eV. Thus the experimental protocol employed during the experiments was suitable to protect the samples from aerial oxidation. As all spectra of tin(II) in Figure 3 are superimposable, it follows that the local structure of tin(II) in these hyperalkaline solutions is identical and independent of the total concentration of both NaOH and tin(II) within the concentration range covered. In the following details will only be given for solution containing 0.05 mol dm<sup>-3</sup> tin(II) in 4 mol·dm<sup>-3</sup> NaOH (Sn5\_4), while data for the rest of the solutions are given in Table 1.

peak related to the primary Sn-O bond distance at  $\sim 2.1 \text{ \AA}$  ( $\sim 1.6 \text{ \AA}$ , not phase corrected). According to this single peak, tin(II) is expected to have a simple local environment, and no multiple scattering from the atoms in the first coordination sphere was detected. This indicates low symmetry around tin(II). Polynuclear tin(II) complexes have not been detected under these conditions as no Sn...Sn pair-interactions are seen on Fourier-transform of the  $k^3$ -weighted EXAFS data. Bond lengths are more accurately determined by EXAFS than the corresponding coordination numbers.<sup>34</sup> The relationship between bond distance and coordination number can therefore in most cases be used to accurately estimate the coordination number from the observed bond distance.<sup>35,36</sup> The  $r_{\text{Sn-O}}$  and  $N$  values of solid O-coordinated tin(II) compounds were collected from the Inorganic Crystal Structure Database and the Cambridge Crystal Structure Database<sup>37,38</sup>, as previously done for lead(II).<sup>39</sup> (The data are given as supplementary information, Table S2) The  $r_{\text{M-O}}$  vs.  $N$  data collected for both metal ions are shown on Figure 4. It is of utmost importance to stress that the spread in the Sn-O bond distances for complexes with the same coordination number and geometry is unusually large, and this is in particular the case for  $N = 3$  (the Sn-O bond lengths are in the range 2.066-2.185  $\text{\AA}$ ). This is most likely due to the stereochemical impact of the occupied anti-bonding orbitals of tin(II). It shall also be mentioned that a mean Sn-O bond distance of 2.080  $\text{\AA}$  in the [Sn(OH)<sub>3</sub>]<sup>-</sup> unit in the solid state has been reported.<sup>40</sup>

The [Sn(OH)<sub>3</sub>]<sup>-</sup> solution complexes was assumed to have trigonal pyramid geometry, with the tin(II) on the top of the pyramid as found for the [Sn(OH)<sub>3</sub>]<sup>-</sup> complex in the solid state<sup>40</sup> and of other three-coordinate tin(II) complexes (Table S2). During the fitting of the EXAFS data,  $N$  was held constant ( $N = 3$ ), and a surprisingly short bond length,  $r_{\text{Sn-O}} = 2.076 \text{ \AA}$ , as well as a small Debye-Waller factor,  $\sigma^2 = 0.0038 \text{ \AA}^2$ , were obtained (Table 1). Former data is in excellent agreement with the bond length observed in the *solid state*.<sup>40</sup> However, it has to be noted that the

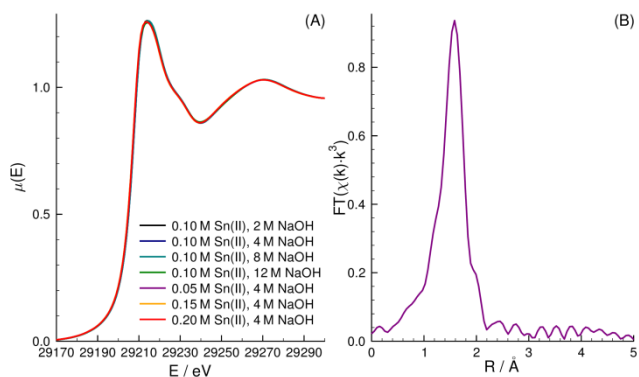


**Fig. 3.** The near-edge region of the alkaline Sn K-edge X-ray absorption spectra of all the alkaline solutions investigated: Sn10\_2, Sn10\_4, Sn10\_8, Sn10\_12, Sn5\_4, Sn15\_4, Sn20\_4 (A) and the Fourier-transform of the  $k^3$ -weighted EXAFS data (B) of sample (Sn5\_4). The acronyms used here are defined in Table 1.

The Fourier transform of the  $k^3$ -weighted EXAFS spectrum is given in Figure 3 (B). This Fourier transform has only a single

value of 2.076 Å is right on the border of ranges for  $N=2$  and  $N=3$ . To confirm the assumption that  $[\text{Sn}(\text{OH})_3]^-$  is the dominating species among these conditions,  $^{119}\text{Sn}$  Mössbauer and Raman spectroscopic measurements as well as quantum chemical calculations were performed.

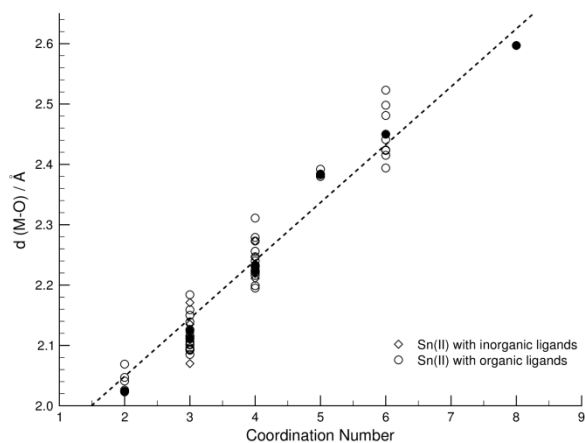


**Fig. 4.** Summary of mean bond distances in tin(II) and compounds (details in Tables S2), and the relationship between the Sn-O bond lengths and the coordination number in various O-coordinated tin(II) compounds. The filled symbols stand for the average values. The dashed line represent the linear trend-line of the mean M-O bond distances as function of coordination number.

Background subtracted FT-Raman spectra of solutions with  $C_{\text{NaOH}} = 4.0$  M and various amounts of Sn(II) are shown in Figure 5. With the increasing Sn(II) concentration, a spectral feature emerges at  $\sim 430$   $\text{cm}^{-1}$  and another, less intense, at  $\sim 490$   $\text{cm}^{-1}$ . Both are due to Sn-O vibrations, as, according to the literature, a broad and weak spectral feature is seen on the Raman trace of SnO,  $\text{Sn}(\text{OH})_2$  and  $\text{SnO}_2$  in the solid state at  $\sim 470$   $\text{cm}^{-1}$ .

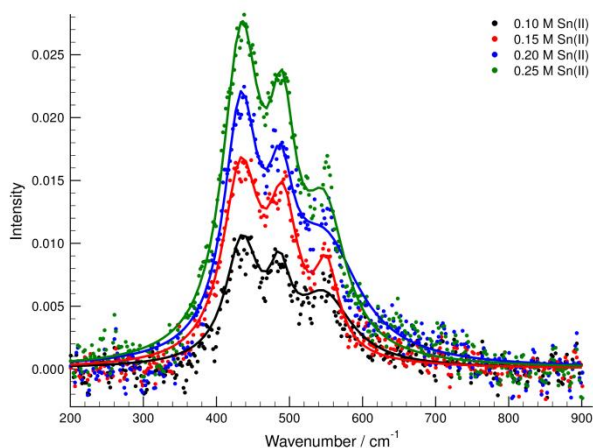


**Fig. 5.** The experimental (markers) and the fitted (lines) Raman spectra of the alkaline solutions with varying  $C_{\text{Sn(II)}}$  at  $C_{\text{NaOH}} = 4$  M.

The peak at  $\sim 580$   $\text{cm}^{-1}$  in Figure 5 is due to formation of Sn(IV) species,<sup>41,44</sup> as its intensity was found increase at the expense of the other two peaks upon bubbling air through the solution. This band is very strong, therefore it causes significant variations in the Raman spectra even if only a few percent of Sn(II) is oxidised to Sn(IV) (Note, that this is inevitable during manipulating the solutions and collecting the spectra). Raman spectra of a more

extended series of solutions with varying composition were also collected. The spectral parameters obtained from them are shown in Table S3. The peak positions ( $\sigma$ ) and peak widths (FWHM) show no major variations with the changing solution composition. The slight increase in  $\sigma$  with the increasing concentration of the base is at the edge of significance (4–6  $\text{cm}^{-1}$ ) and is most probably associated with formation of contact ion pairs.<sup>7</sup> The Raman parameters obtained in media containing potassium instead of sodium are practically identical. The height is roughly linearly proportional to the total concentration of Sn(II) (Figure S2). These observations suggest, that there is only one Sn(II)-containing species present in these solutions, the composition and structure of which is independent of the concentration of the solutes.

For *ab initio* calculations, a piano chair like (trigonal pyramid) structure was assumed for the  $[\text{Sn}(\text{OH})_3]^-$  and a V-shaped arrangement for the  $[\text{SnO}(\text{OH})]^-$ . The primary Sn–O bond lengths were found to be 2.05 Å and 1.86 and 2.06 Å for the three- and two coordinated complex, respectively. Raman spectra of these species have been calculated (Figure 6). On the calculated spectra of both species, peaks are seen at around 430 and 490  $\text{cm}^{-1}$ , with larger intensity corresponding to the band at the smaller wavenumber. The same can be observed on the experimental spectrum. The striking difference is, that the most intense calculated peak corresponding to  $[\text{SnO}(\text{OH})]^-$  is found at 700  $\text{cm}^{-1}$ , which is completely missing from the observed spectra (Figure 5), strongly suggesting, that the observed spectrum corresponds to the three-coordinated complex,  $[\text{Sn}(\text{OH})_3]^-$ .

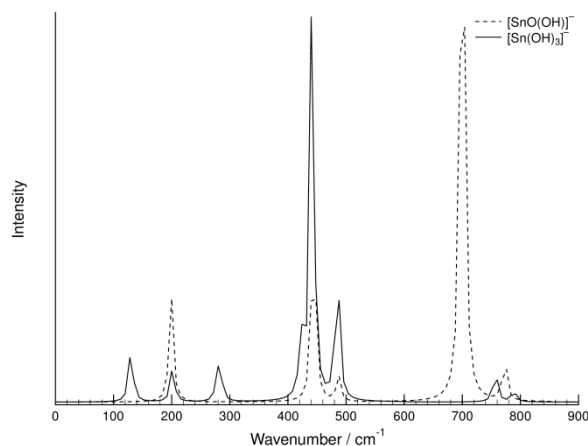


**Fig. 6.** Calculated Raman spectra of  $[\text{Sn}(\text{OH})_3]^-$  and  $[\text{SnOOH}]^-$ , respectively

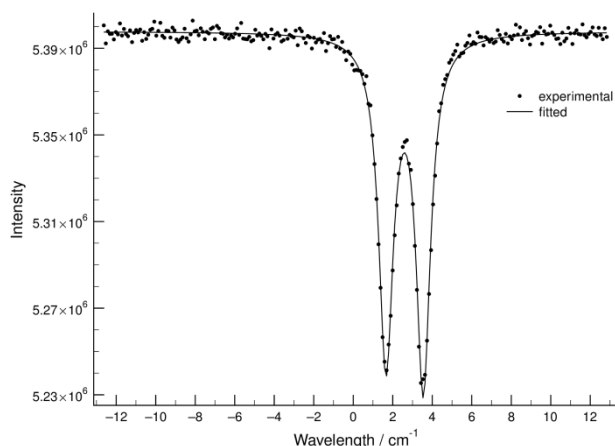


**Fig. 7.**  $^{119}\text{Sn}$  Mössbauer spectrum, of a representative frozen solution with  $C_{\text{Sn(II)}} = 0.2 \text{ M}$  and  $C_{\text{NaOH}} = 4 \text{ M}$  ( $T = 20\text{K}$ ).

The  $^{119}\text{Sn}$  Mössbauer spectrum (Figure 7) consists of a slightly asymmetric doublet with  $IS = 2.69 \text{ mm/s}$  and  $QS = 2.06 \text{ mm/s}$ . These Mössbauer parameters are in the range of those found for  $\text{Sn(OH)}_2$  ( $IS = 2.95 \text{ mm/s}$  and  $QS = 2.16 \text{ mm/s}$ )<sup>45</sup> as well as  $\text{SnO}$  ( $IS = 2.8 - 3.4 \text{ mm/s}$  and  $QS = 1.3 - 2.28 \text{ mm/s}$ )<sup>46-49</sup> and reported in the literature. No significant change was found in the Mössbauer parameters of this doublet when the concentration of  $\text{Sn(II)}$  or  $\text{NaOH}$  was changed (Table S4). Since the hyperfine interactions detected by the Mössbauer spectroscopy are mostly affected by the first coordination sphere of  $\text{Sn}$ , mainly the effect of oxygen nearest neighbour environment of  $\text{Sn(II)}$  can be detected in the alkaline solutions, which remains unchanged with changing solution composition.  $QS$  values were calculated according to literature procedures<sup>50</sup> both for  $[\text{Sn(OH)}_3]^-$  and for  $[\text{SnO(OH)}]^-$ . It was found, that the calculated  $QS$  value for the  $[\text{SnO(OH)}]^-$  complex was much larger ( $3.11 \text{ mm/s}$ ) than the experimentally found. The calculated  $QS$  value for  $[\text{Sn(OH)}_3]^-$  was  $2.62 \text{ mm/s}$ . The  $IS$  ( $2.72 \text{ mm/s}$ ) and  $QS$  ( $2.26$ ) values<sup>51</sup> obtained for the solid  $\text{NaSn(OH)}_3$  are also very similar to those found by us, however, the local structure of  $\text{Sn(II)}$  in this compound is not established. Based on the analogy between  $\text{F}^-$  and  $\text{OH}^-$ , it is remarkable, that the  $QS$  values for  $\text{MSnF}_3$  compounds ( $\text{M}^+ = \text{Na}^+, \text{K}^+, \text{Rb}^+$  and  $\text{Cs}^+$ )<sup>52</sup> are in the range of  $1.84 - 2.00 \text{ mm/s}$ , while  $QS = 2.15 \text{ mm/s}$  for  $\text{SnF}_2$ .<sup>53</sup> In  $\text{SnF}_2$ , from single crystal X-ray diffraction experiments, the  $\text{Sn(II)}$  ion is in trigonal pyramidal environment.<sup>54</sup>

## Conclusions

In summary, EXAFS spectroscopic measurements show that only one kind of tin(II) complex is present in strongly alkaline aqueous solutions, containing  $0.1 - 12.0 \text{ mol-dm}^{-3}$  hydroxide. The predominating complex is mononuclear with surprisingly short  $\text{Sn-O}$  bond length,  $2.078 \text{ \AA}$ , which is within the range of bond distances observed for tin(II) complexes coordinated by three oxygens. The presence of chloride ions, even in high concentrations, has no effect on the local structure of the complex as proven by the XAS measurements. The  $\text{Sn(II):OH}^-$  ratio is unambiguously 1:3 from potentiometric titrations using  $\text{H}_2/\text{Pt}$  electrode. These observations together with Raman and

Mössbauer spectroscopic results and *ab initio* quantum chemical calculations fully support the exclusive (or at least overwhelmingly predominant) presence of the mononuclear  $[\text{Sn(OH)}_3]^-$  complex in these hyper-alkaline aqueous solutions.

## Acknowledgment

Research leading to this contribution was supported by the National Research Fund of Hungary through OTKA 83889. The X-ray absorption measurements were supported by the CALIPSO (TNA, European Union) program. Éva G. Bajnóczi would like to thank the Campus Hungary Scholarship of the Balassi Institute which financed a five week short term study at the Department of Chemistry, Swedish University of Agricultural Sciences, Uppsala, Sweden. Great thanks to Valérie Briois, beamline scientist at SAMBA, Soleil, for her essential help during the X-ray absorption measurements.

## Notes and references

- <sup>a</sup> Department of Inorganic and Analytical Chemistry, University of Szeged, H-6720 Dóm tér 7., Szeged, Hungary
- <sup>b</sup> Laboratory of Nuclear Chemistry, Institute of Chemistry, Eötvös Loránd University, Budapest H-1117, Hungary
- <sup>c</sup> Institute of Molecular Pharmacology, Research Centre for Natural Sciences, Hungarian Academy of Sciences, Pusztaszeri út 59-67, H-1025 Budapest, Hungary
- <sup>d</sup> Institute of Pharmaceutical Analysis, University of Szeged, Somogyi u. 4, Szeged H-6720, Hungary
- <sup>e</sup> Department of Physical Chemistry and Materials Science, University of Szeged, H-6720 Aradi vértanúk tere 1., Szeged, Hungary
- <sup>f</sup> Department of Organic Chemistry, University of Szeged, H-6720 Dóm tér 8., Szeged, Hungary
- <sup>g</sup> Department of Chemistry and Biotechnology, Swedish University of Agricultural Sciences, SE-750 07, Uppsala, Sweden
- <sup>h</sup> Materials and Solution Structure Research Group, Institute of Chemistry, University of Szeged H-6720 Aradi vértanúk tere 1., Szeged, Hungary
- <sup>i</sup> Corresponding authors: [sipos@chem.u-szeged.hu](mailto:sipos@chem.u-szeged.hu), [Ingmar.persson@slu.se](mailto:Ingmar.persson@slu.se)
- <sup>†</sup> Electronic Supplementary Information (ESI) available: [details of any supplementary information available should be included here]. See DOI: 10.1039/b000000x/
- Pallagi, É. G. Bajnóczi, S. E. Canton, T. B. Bolin, G. Peintler, B. Kutus, Z. Kele, I. Palinko, P. Sipos, *Env. Sci. Technol.* 2014, **48**, 6604-6611.
- Pallagi, Á. G. Tasi, G. Peintler, P. Forgo, I. Palinko, P. Sipos, *Dalton Trans.* 2013, **42**, 13470-13476.
- E. Horváth, Á. Kukovecz, Z. Kónya, I. Kiricsi, *Chem. Mater.* 2007, **4**, 927-931.
- D. Srankó, A. Pallagi, E. Kuzmann, S. E. Canton, M. Walczak, A. Sági, A. Kukovecz, Z. Kónya, P. Sipos, I. Palinko, *Appl. Clay Sci.* 2010, **48**, 214-217.
- E. Martell; R. M. Smith, *Critical Stability Constants*; Plenum Press: London, 1975.
- F. Baes, R. E. Mesmer, *The Hydrolysis of Cations*, John Wiley & Sons: New York, 1976; ch 15.3.
- P. Sipos, *J. Mol. Liq.* 2010, **146**, 1-14.
- P. Sipos, P. M. May, G. Hefter, *Dalton Trans.*, 2006, 368-375
- R. Buchner, P. Sipos, G. Hefter, P. M. May, *J. Phys. Chem., A* 2002, **106**, 6527-6532.
- P. Sipos, T. Megyes, O. Berkesi, *J. Soln. Chem.* 2008, **34**, 1411-1418.
- T. Radnai, Sz. Bálint, I. Bakó, T. Megyes, T. Grósz, A. Pallagi, G. Peintler, I. Palinko, P. Sipos, *Phys. Chem. Chem Phys.* 2014, **16**, 4023-4032.

- 12 N. Tarapova, A. Radkevich, D. Davydov, A. Titov, I. Persson, *Inorg. Chem.*, 2009, **48**, 10383-10388.
- 13 Zydorczak, P. M. May, D. P. Meyrick, D. Batka, G. T. Hefter, *Ind. Eng. Chem. Res.* 2012, **51**, 16537-16543.
- 5 14 N. Perera, G. T. Hefter, P. Sipos, *Inorg. Chem.* 2001, **40**, 3974-3978.
- 15 P. Sipos, S. G. Capewell, P. M. May, G. T. Hefter, G. Laurenczy, F. Lukács, R. Roulet, *J. Solution Chem.* 1997, **26**, 419-431.
- 16 P. Sipos, S. G. Capewell, P. M. May, G. T. Hefter, G. Laurenczy, F. Lukács, R. Roulet, *J. Chem. Soc., Dalton Trans.* 1998, 3007-3012.
- 10 17 M. Navarro, P. M. May, G. Hefter, E. Königsberger, *Hydrometallurgy* 2014, **147-148**, 68-72.
- 18 P. Sipos, D. Zeller, E. Kuzmann, A. Vértes, Z. Homonnay, M. Walczak, S. Canton, *Dalton Trans.* 2008, 5603-5611.
- 19 M. Altmaier, X. Gaona, T. Fenghanel, *Chem. Rev.* 2013, **113**, 901-943.
- 15 20 R. M. Cigala, F. Crea, C. De Stefano, G. Lando, D. Milea and S. Sammartano, *Geochim. Cosmochim. Acta*, 2012, **87**, 1-20.
- 21 F. Séby, M. Potin-Gautier, E. Giffaut, and O. F. X. Donard, *Geochim. Cosmochim. Acta*, 2001, **65**, 3041-3053.
- 20 22 H. Gamsjäger, T. Gajda, J. Sangster, S. K. Saxena, W Voigt, *Chemical Thermodynamics*; ed. J. Perrone, OECD Publishing: 2012; vol 12, ch 7.
- 23 W. Mark, *Acta Chem. Scand. A* 1977, **31**, 157-162.
- 24 F. A. Cotton and G. Wilkinson, *Advanced Inorganic Chemistry*, Wiley Interscience, New York, USA, 1988, p. 296.
- 25 25 P. Sipos, G. T. Hefter, P. M. May, *J. Chem. Eng. Data* 2000, **45**, 613-616.
- 26 P. Sipos, G. T. Hefter, P. M. May, *The Analyst*, 2000, **125**, 955-958.
- 27 P. Sipos, G. T. Hefter, P. M. May, *Aust. J. Chem.* 1998, **51**, 445-454.
- 30 28 P. Sipos, M. Schibeci, G. Peintler, P. M. May, G. T. Hefter, *Dalton Trans.* 2006, 1858-1866.
- 29 Thompson, D. Attwood, E. Gullikson, M. Howells, K-J. Kim, J. Kirz, J. Kortright, I. Lindau, Y. Liu, P. Pianetta, A. Robinson, J. Scofield, J. Underwood, G. Williams, H. Winick, X-ray data booklet, Lawrence Berkley National Laboratory, 2009.
- 35 30 G. N. George, I. F. Pickering, EXAFSPAK - A suite of Computer Programs for Analysis of X-ray absorption spectra, Stanford Synchrotron Radiation Laboratory, Stanford, CA, 1995. <http://www-ssl.slac.stanford.edu/exafspak.html> (accessed July 2014)
- 40 31 S. I. Zabinsky, J. J. Rehr, A. Ankudinov, R. C. Albers, M. Eller, *Phys. Rev. B*, 1995, **52**, 2995-3009.
- 32 Z. Klencsár, E. Kuzmann, A. Vértes, *J. Radioanal. Nucl. Chem.* 1996, **201**, 105-118.
- 45 33 M. Sherman, K. V. Ragnarsdottir, E. H. Oelkers, C. R. Collins, *Chem. Geol.* 2000, **167**, 169-176.
- 34 Persson, M. Sandström, H. Yokoyama, M. Chaudhry, *Z. Naturforsch., Sect. A* 1995, **50**, 21-37.
- 35 R. D. Shannon, *Acta Crystallogr., Sect. A* 1976, **32**, 751-767.
- 50 36 Lundberg, I. Persson, L. Eriksson, P. D'Angelo, S. De Panfilis, *Inorg. Chem.* 2010, **49**, 4420-4432.
- 37 F. H. Allen, *Acta Crystallogr., Sect. B* 2002, **58**, 380-388.
- 38 Inorganic Crystal Structure Database; FIZ Karlsruhe, 2013.
- 39 Persson, K. Lyczko, D. Lundberg, L. Eriksson, A. Płaczek, *Inorg. Chem.* 2011, **50**, 1058-1072, and references therein.
- 55 40 von H. G. Schnering, R. Nesper, H. Pelshenke, *Z. Anorg. Allg. Chem.* 1983, **499**, 117-129.
- 41 X. Huang, P. Tornatore, Y.-S. Li, *Electrochim. Acta*, 2000, **46**, 671-679.
- 60 42 M. Ocana, C. J. Serna, J. V. Garcia-Ramos, *Solid State Ionics* 1993, **63**, 170-177.
- 43 Zou, C. Xu, X. Liu, C. Wang, *J. Appl. Phys.* 1994, **75**, 1835-1836.
- 44 Nakamoto, *Infrared and Raman Spectra of Inorganic and Coordination Compounds*, John Wiley & Sons, New York, 1997
- 65 45 N. Alberola, *Polyhedron*, 1985, **4**, 1853-1857.
- 46 P. A. Cusack, P. J. Smith, W. J. Kroenke, *Polym. Degr. Stab.*, 1986, **14**, 307-318.
- 47 S. Ichiba, M. Takeshita, *Bull. Chem. Soc. Jpn.*, 1984, **57**, 1087-1091.
- 48 P. E. Lippens, *Phys. Rev. B*, 1999, **60**, 4576-4590.
- 70 49 P. S. Cook, J. D. Cashion, P. J. Cassidy, *Fuel*, 1985, **8**, 1121-1126.
- 50 G. Barone, A. Silvestri, G. Ruisi, G. La Manna, *Chem. Eur. J.*, 2005, **11**, 6185-6191.
- 51 W. Thornton, P. G. Harrison, *J. Chem. Soc., Faraday Trans.*, 1975, **71**, 461-472.
- 75 52 R. V. Paris, *Structure and Bonding in Tin Compounds*, in G. J. Long, *Mössbauer Spectroscopy Applied to Inorganic Chemistry*, Plenum Press, New York and London, 1984 and the references cited therein.
- 53 G. Ballard, T. Birchall, *Can. J. Chem.*, 1975, **53**, 3371-3373.
- 80 54 R. C. McDonald, H. H.-K. Hau, K. eriks, *Inorg. Chem.*, 1976, **15**, 762-765.

# Speciation and structure of tin(II) in hyper-alkaline aqueous solution

Éva G. Bajnóczi,<sup>a,h</sup> Eszter Czeglédi,<sup>a,h</sup> Ernő Kuzmann,<sup>b</sup> Zoltán Homonnay,<sup>b</sup> Szabolcs Bálint,<sup>c</sup> György Dombi,<sup>d</sup> Péter Forgo,<sup>d</sup> Ottó Berkesi,<sup>e</sup> István Pálinkó,<sup>f,h</sup> Gábor Peintler,<sup>e,h</sup> Pál Sipos,<sup>a,h\*</sup> and Ingmar Persson<sup>g\*</sup>

<sup>a</sup> *Department of Inorganic and Analytical Chemistry, University of Szeged, H-6720 Dóm tér 7., Szeged, Hungary*

<sup>b</sup> *Laboratory of Nuclear Chemistry, Institute of Chemistry, Eötvös Loránd University, Budapest H-1117, Hungary*

<sup>c</sup> *Institute of Molecular Pharmacology, Research Centre for Natural Sciences, Hungarian Academy of Sciences, Pusztaszeri út 59-67, H-1025 Budapest, Hungary*

<sup>d</sup> *Institute of Pharmaceutical Analysis, University of Szeged, Somogyi u. 4, Szeged H-6720, Hungary*

<sup>e</sup> *Department of Physical Chemistry and Materials Science, University of Szeged, H-6720 Aradi vértanúk tere 1., Szeged, Hungary*

<sup>f</sup> *Department of Organic Chemistry, University of Szeged, H-6720 Dóm tér 8., Szeged, Hungary*

<sup>g</sup> *Department of Chemistry and Biotechnology, Swedish University of Agricultural Sciences, SE-750 07, Uppsala, Sweden*

<sup>h</sup> *Materials and Solution Structure Research Group, Institute of Chemistry, University of Szeged H-6720 Aradi vértanúk tere 1., Szeged, Hungary*

**Electronic Supplementary Information**

**Table S1.** Summary of solid state structures containing trichlorostannate,  $[\text{SnCl}_3]^-$  or tetrachlorostannate,  $[\text{SnCl}_4]^{2-}$  complexes. The list is based on the data collected from the Inorganic Crystal Structure Database (ICSD) and the Cambridge Structural Database (CSD).

***Trichlorostannate(II)***

ICSD/CSD code	$d_{\text{Sn-Cl}}$	Reference
PECOTB20	2.430 Å	Stalick, J. K.; Corfield, P. W. R; Meek, D. W. <i>Inorg. Chem.</i> <b>1973</b> , <i>12</i> , 1668.
PPECOT20	2.445 Å	Stalick, J. K.; Corfield, P. W. R; Meek, D. W. <i>Inorg. Chem.</i> <b>1973</b> , <i>12</i> , 1668.
DOWKIJ	2.453 Å	Fong, L. K.; Fox, J. R.; Foxman, B. M.; Cooper, N. J. <i>Inorg. Chem.</i> <b>1986</b> , <i>25</i> , 1880.
BIWLUP	2.466 Å	Hernandez-Molina, R.; Kalinina, I. V.; Abramov, P. A.; Sokolov, M. N.; Virovets, A. V.; Platas J. G.; Llusar, R.; Polo, V.; Vicent, C.; Fedin, V. P. <i>Inorg. Chem.</i> <b>2008</b> , <i>47</i> , 306.
SIGMEA	2.467 Å	Veith, M.; Godicke, B.; Huch, V. <i>Z. Anorg. Allg. Chem.</i> <b>1989</b> , <i>579</i> , 99.
VOGRAK	2.467 Å	Balch, A. L.; Neve, F.; Olmstead, M. M. <i>Inorg. Chem.</i> <b>1991</b> , <i>30</i> , 3395.
240910	2.468 Å	Szafranski, M.; Ståhl, K. <i>J. Solid State Chem.</i> <b>2007</b> , <i>180</i> , 2209-2215.
XETZUS	2.471 Å	Muller, U.; Mronga, N.; Schumacher, C.; Dehnicke, K. <i>Z. Naturforsch., Teil B</i> <b>1982</b> , <i>37</i> , 1122.
NAKPUK	2.474 Å	Constantine, S. P.; De Lima, G. M.; Hitchcock, P. B.; Keates, J. M.; Lawless, G. A. <i>Chem. Commun.</i> <b>1996</b> , 2337.
LAQVUU	2.480 Å	Faure, J.-L.; Gornitzka, H.; Reau, R.; Stalke, D.; Bertrand, G. <i>Eur. J. Inorg. Chem.</i> <b>1999</b> , 2295.
DUSWOD	2.481 Å	Drew, M. G. B.; Nicholson, D. G. <i>J. Chem. Soc., Dalton Trans.</i> <b>1986</b> , 1543.
SIGNIF	2.486 Å	Veith, M.; Godicke, B.; Huch, V. <i>Z. Anorg. Allg. Chem.</i> <b>1989</b> , <i>579</i> , 99.
ENCOSN	2.488 Å	Haupt, H. J.; Huber, F.; Preut, H. <i>Z. Anorg. Allg. Chem.</i> <b>1976</b> , <i>422</i> , 255.
KAYJOJ	2.500 Å	Hough, E.; Nicholson, D. G.; Vasudevan, A. K. <i>J. Chem. Soc., Dalton Trans.</i> <b>1989</b> , 2155.
170096	2.505 Å	Halfpenny, J. <i>Acta Crystallogr., Sect. C</i> <b>1996</b> , <i>52</i> , 340-342.
GIYGOK	2.507 Å	Kuhn, N.; Fawzi, R.; Kotowski, H.; Steimann, M. <i>Z. Kristallogr.-New Cryst. Struct</i> <b>1998</b> , <i>213</i> , 435.
KAHWAR	2.515 Å	Veith, M.; Huch, V.; Lisowsky, R.; Hobein, P. <i>Z. Anorg. Allg. Chem.</i> <b>1989</b> , <i>569</i> , 43.
14199	2.523 Å	Poulsen, F. R.; Rasmussen, S. E. <i>Acta Chem. Scand.</i> <b>1970</b> , <i>24</i> , 150-156.
BZSACS	2.527 Å	Elder, R. C.; Heeg, M. J.; Deutsch, E. <i>Inorg. Chem.</i> <b>1978</b> , <i>17</i> , 427.
GEHTUI	2.542 Å	Veith, M.; Jarczyk, M.; Huch, V. <i>Chem. Ber.</i> <b>1988</b> , <i>121</i> , 347.
30171	2.559 Å	Harrison, P. G.; Haylett, B. J.; King, T. J. <i>Inorg. Chim. Acta</i> <b>1983</b> , <i>75</i> , 265-270.
110664	2.567 Å	Yamada, K.; Kuranaga, Y.; Ueda, K.; Goto, S.; Okuda, T.; Furukawa, Y. <i>Bull. Chem. Soc. Jpn.</i> <b>1998</b> , <i>71</i> , 127-134.
14219	2.571 Å	Kamenar, B.; Grdenic, D. <i>J. Inorg. Nucl. Chem.</i> <b>1962</b> , <i>24</i> , 1039-1045.

1363	2.603 Å	Haupt, H. J.; Huber, F.; Sandbote, H. W. <i>Z. Anorg. Allgem. Chem.</i> <b>1977</b> , 435, 191-196.
32593	2.605 Å	Golic, L.; Kaucic, V.; Trontelj, Z. <i>Docum. Chem. Yugoslav. Vestnik Sloven. Kemi. Drustva</i> <b>1979</b> , 26, 425-434.
415711	2.610 Å	Abraham, I.; Demetriou, D. Z.; Vordemvenne, E.; Mustarde, K.; Benoit, D. M. <i>Polyhedron</i> <b>2006</b> , 25, 996-1002.
110663	2.637 Å	Yamada, K.; Kuranaga, Y.; Ueda, K.; Goto, S.; Okuda, T.; Furukawa, Y. <i>Bull. Chem. Soc. Jpn.</i> <b>1998</b> , 71, 127-134.
<b>Average</b>	<b>2.513 Å/27 structures</b>	

#### ***Tetrachlorostannate(II)***

VIZJET	2.634 Å	Sokol, V. I.; Vasilenko, T. G.; Porai-Koshits, M. A.; Molodkin, A. K.; Vasnin, S. V. <i>Zh. Neorg. Khim.</i> <b>1990</b> , 35, 2017.
<b>Average</b>	<b>2.634 Å/1 structure</b>	

**Table S2** The oxygen coordinated tin(II) structures used for determine the coordination number – Sn-O bond distance relationship for coordination numbers = 2, 3, 4, 5, 6, 8. The list is based on the data collected from the Inorganic Crystal Structure Database (ICSD) and the Cambridge Structural Database (CSD); *N* = coordination number; references marked in red text are omitted from the mean bond distance and angle.

<i>N</i>	CSD code	$d_{\text{Sn-O}}$	$\angle\text{O-Sn-O}$	Reference
2	BOSSIM	1.964 Å	99.5°	Nembenna, S.; Singh, S.; Jana, A.; Roesky, H. W.; Ying Yang, Hongqi Ye; Ott, H.; Stalke, D. <i>Inorg. Chem.</i> <b>2009</b> , 48, 2273.
2	PAQHYY	1.992 Å	95.6°	Hascall, T.; Rheingold, A. L.; Guzei, I.; Parkin, G. <i>Chem. Commun.</i> <b>1998</b> , 101.
2	HEBXOB	2.024 Å	88.8°	Barnhart, D. M.; Clark, D. L.; Watkin, J. G. <i>Acta Crystallogr., Sect. C</i> 1994, 50, 702.
2	HEBXOB01	2.026 Å	89.0°	Boyle, T. J.; Doan, T. Q.; Steele, L. A. M.; Aplett, C.; Hoppe, S. M.; Hawthorne, K.; Kalinich, R. M.; Sigmund, W. M. <i>Dalton Trans.</i> <b>2012</b> , 41, 9349.
2	LIXLUA	2.041 Å	87.3°	Dickie, D. A.; MacIntosh, I. S.; Ino, D. D.; Qi He; Labeodan, O. A.; Jennings, M. C.; Schatte, G.; Walsby, C. J.; Clyburne, J. A. C. <i>Can. J. Chem.</i> <b>2008</b> , 86, 20.
2	PEBVIC	2.047 Å	92.2°	Stanciu, C.; Richards, A. F.; Stender, M.; Olmstead, M. M.; Power, P. P. <i>Polyhedron</i> <b>2006</b> , 25, 477.

2	NINSIN	2.069 Å	89.4 °	Hascall, T.;Keliang Pang;Parkin, G. <i>Tetrahedron</i> <b>2007</b> , 63, 10826.	
2	JOQBOG	2.104 Å	73.0 °	McBurnett, B. G.; Cowley A. H. <i>Chem. Commun.</i> <b>1999</b> , 17.	
<b>Average</b>		<b>2.023 Å/7 structures</b>			
2	DASJEM			Fjeldberg, T.; Hitchcock, P. B.; Lappert, M. F.; Smith, S. J.; Thorne, A. J. <i>Chem. Commun.</i> <b>1985</b> , 939.	
2	TBMGEB			Cetinkaya, B.; Gumrukcu, I.; Lappert, M. F.; Atwood, J. L.; Rogers, R. D.; Zaworotko, M. J. <i>J. Am. Chem. Soc.</i> <b>1980</b> , 102, 2088.	
3	Na <sub>4</sub> [Sn(OH) <sub>3</sub> ] <sub>2</sub> . [Sn <sub>2</sub> O(OH) <sub>4</sub> ]	35420	2.080 Å	88.1 °	von Schnering, H.G.; Nesper, R.; Pelshenke, H. <i>Z. Anorg. Allgem. Chem.</i> <b>1983</b> , 499, 117-129
3	Na <sub>4</sub> [Sn(OH) <sub>3</sub> ] <sub>2</sub> . [Sn <sub>2</sub> O(OH) <sub>4</sub> ]	35420	2.066 Å	89.3 °	von Schnering, H.G.; Nesper, R.; Pelshenke, H. <i>Z. Anorg. Allgem. Chem.</i> <b>1983</b> , 499, 117-129
3	Sn <sub>3</sub> O(OH) <sub>2</sub> (SO <sub>4</sub> )	4294	2.122 Å	89.2 °	Grimvall, S. <i>Acta Chem. Scand., Ser. A</i> <b>1975</b> , 29, 590-598.
3	Sn <sub>3</sub> O(OH) <sub>2</sub> (SO <sub>4</sub> )	15778	2.127 Å	89.6 °	Davies, C. G.; Donaldson, J. D.; Laughlin, D. R.; Howie, R. A.; Beddoes, R. <i>J. Chem. Soc., Dalton Trans.</i> , <b>1975</b> , 2241-2244.
3	Sn <sub>3</sub> O(OH)(PO <sub>4</sub> )	23339	2.135 Å	83.8 °	Jordan, T. H.; Dickens, B.; Schroeder, L. W.; Brown, W. E. <i>Inorg. Chem.</i> <b>1980</b> , 19, 2551-2556.
3	Sn <sub>3</sub> O(OH)(PO <sub>4</sub> )	23339	2.171 Å	84.8 °	Jordan, T. H.; Dickens, B.; Schroeder, L. W.; Brown, W. E. <i>Inorg. Chem.</i> <b>1980</b> , 19, 2551-2556.
<b>Average</b>		<b>2.117 Å</b>	<b>87.5 °/6 structures</b>		
4	SnO	26597	2.211 Å	89.2 °	Moore, W. J.; Pauling, L. <i>J. Am. Chem. Soc.</i> <b>1941</b> , 63, 1392-1394.
4	SnO	15516	2.219 Å	88.9 °	Izumi, F. <i>J. Solid State Chem.</i> <b>1981</b> , 38, 381-385.
4	SnO	41954	2.222 Å	88.8 °	Moreno, M. S.; Mercader, R. C. <i>Phys. Rev. B</i> <b>1994</b> , 50, 9875-9881.
4	SnO	16481	2.224 Å	88.8 °	Pannetier, J.; Denes, G. <i>Acta Crystallogr., Sect. B</i> <b>1980</b> , 36, 2763-2765.

4	SnO	185350	2.224 Å	88.7 °	Allen, J. P.; Scanlon, D. O.; Parker, S. C.; Watson, G. W. <i>J. Phys. Chem. C</i> <b>2011</b> , <i>115</i> , 19916-19924.
4	Sn <sub>3</sub> O(OH)(PO <sub>4</sub> )	23339	2.246 Å	91.6 °	Jordan, T. H.; Dickens, B.; Schroeder, L. W.; Brown, W. E. <i>Inorg. Chem.</i> <b>1980</b> , <i>19</i> , 2551-2556.
4	Sn <sub>3</sub> O(OH) <sub>2</sub> O(SO <sub>4</sub> )	15778	2.273 Å	89.3 °	Davies, C. G.; Donaldson, J. D.; Laughlin, D. R.; Howie, R. A.; Beddoes, R. <i>J. Chem. Soc., Dalton Trans.</i> , <b>1975</b> , 2241-2244.

**Average**                      **2.224 Å**    **89.3 °/6 structures**

<i>N</i>	CSD code	<i>d</i> <sub>Sn-O</sub>	∠O-Sn-O	Reference
3	FEKTOF	2.085 Å	85.0 °	Veith, M.; Ehses, M.; Huch, V. <i>New J. Chem.</i> <b>2005</b> , <i>29</i> , 154-164.
3	DUVNIR	2.092 Å	88.8 °	Veith, M.; Rosler, R. <i>Z. Naturforsch., Teil B</i> <b>1986</b> , <i>41</i> , 1071.
3	DEPQEV	2.093 Å	86.6 °	Ramaswamy, P.; Natarajan, S. <i>Eur. J. Inorg. Chem.</i> <b>2006</b> , 3463-3471.
3	DUVNOX	2.094 Å	87.1 °	Veith, M.; Rosler, R. <i>Z. Naturforsch., Teil B</i> <b>1986</b> , <i>41</i> , 1071.
3	FEKTUL	2.096 Å	85.5 °	Veith, M.; Ehses, M.; Huch, V. <i>New J. Chem.</i> <b>2005</b> , <i>29</i> , 154-164.
3	DASHUA	2.101 Å	79.7 °	Fjeldberg, T.; Hitchcock, P. B.; Lappert, M. F.; Smith, S. J.; Thorne, A. J. <i>J. Chem. Soc., Chem. Commun.</i> <b>1985</b> , 939-941.
3	JIYPIQ	2.102 Å	79.3 °	Ayyappan, S.; Bu, X.; Cheetham, A. K.; Natarajan, S.; Rao, C. N. R. <i>Chem. Commun.</i> <b>1998</b> , 2181-2182.
3	DUVNOX	2.106 Å	86.8 °	Veith, M.; Rosler, R. <i>Z. Naturforsch., Teil B</i> <b>1986</b> , <i>41</i> , 1071.
3	JOTHOP	2.111 Å	86.9 °	Natarajan, S.; Eswaramoorthy, M.; Cheetham, A. K.; Rao, C. N. R. <i>Chem. Commun.</i> <b>1998</b> , 1561-1562.
3	BIFJOQ	2.115 Å	86.0 °	Duchateau, R.; Dijkstra, T. W.; Severn, J. R.; van Santen, R. A.; Korobkov, I. V. <i>Dalton Trans.</i> <b>2004</b> , 2677-2682.
3	GIVDOE	2.116 Å	86.5 °	Ayyappan, S.; Cheetham, A. K.; Natarajan, S.; Rao, C. N. R. <i>J. Solid State Chem.</i> <b>1998</b> , <i>139</i> , 207-210.
3	JOQBEW	2.126 Å	80.9 °	McBurnett, B. G.; Cowley, A. H. <i>Chem. Commun.</i> <b>1999</b> , 17-18.
3	JOQBEW	2.139 Å	80.0 °	McBurnett, B. G.; Cowley, A. H. <i>Chem. Commun.</i> <b>1999</b> , 17-18.
3	KAFHEE	2.150 Å	76.0 °	Smith, G. D.; Fanwick, P. E.; Rothwell, I. P. <i>Inorg. Chem.</i> <b>1989</b> , <i>28</i> , 618-620.

3	BIDWIV	2.159 Å	84.9 °	Reuter, H. Z. <i>Kristallogr.-New Cryst. Struct.</i> <b>2004</b> , 219, 109-110.
3	COHVEA	2.184 Å	79.4 °	Arifin, A.; Filmore, E. J.; Donaldson, J. D.; Grimes, S. M. <i>J. Chem. Soc., Dalton Trans.</i> <b>1984</b> , 1965-1968.
	<b>Average:</b>	<b>2.112 Å</b>	<b>84.0 °</b>	<b>/15 structures</b>

<i>N</i>	CSD code	$d_{\text{Sn-O}}$	$\angle\text{O-Sn-O}$	Reference
4	SUXLAY	2.195 Å	89.0 °	Barret, M. C.; Mahon, M. F.; Molloy, K. C., Steed, J. W.; Wright, P. <i>Inorg. Chem.</i> <b>2001</b> , 40, 4384-4388.
4	YERBON	2.199 Å	97.2 °	Ionkin, A. S.; Marshall, W. J.; Fish, B. M. <i>Organometallics</i> <b>2006</b> , 25, 4170-4178.
4	PBONSN	2.216 Å	94.2 °	Ewings, P. F. R.; Harrison, P. G.; King, T. J. <i>J. Chem. Soc., Dalton Trans.</i> <b>1975</b> , 1455-1458.
4	SIHQOP	2.221 Å	90.4 °	Ayyappan, S.; Cheetham, A. K.; Natarajan, S.; Rao, C. N. R. <i>Chem. Mater.</i> <b>1998</b> , 10, 3746-3755.
4	WIDCAN	2.221 Å	92.2 °	Pettinari, C.; Marchetti, F.; Cingolani, A.; Marciante, C.; Spagna, R.; Colapietro, M. <i>Polyhedron</i> <b>1994</b> , 13, 939-950.
4	XEXSUP	2.222 Å	83.5 °	Piskunov, A. V.; Lado, A. V.; Fukin, G. K.; Baranov, E. V.; Abakumova, L. G.; Cherkasov, V. K.; Abakumov, G. A. <i>Heteroat. Chem.</i> <b>2006</b> , 17, 481-490.
4	SUXKUR	2.225 Å	91.9 °	Barret, M. C.; Mahon, M. F.; Molloy, K. C., Steed, J. W.; Wright, P. <i>Inorg. Chem.</i> <b>2001</b> , 40, 4384-4388.
4	ABIBIX	2.230 Å	91.3 °	Pettinari, C.; Marchetti, F.; Pettinari, R.; Cingolani, A.; Rivarola, E.; Phillips, C.; Tanski, J.; Rossi, M.; Caruso, F. <i>Eur. J. Inorg. Chem.</i> , <b>2004</b> , 3484-3497.
4	DPPRSN	2.231 Å	90.7 °	Uchida, T.; Kozawa, K.; Obara, H. <i>Acta Crystallogr., Sect. B.</i> <b>1977</b> , 33, 3227-3229.
4	KSNOXL	2.233 Å	88.9 °	Christie, A. D.; Howie, R.A.; Moser, W. <i>Inorg. Chim. Acta</i> <b>1979</b> , 36, L447-L448.
4	AGEBIX	2.240 Å	98.0 °	Boyle, T. J.; Alam, T. M.; Rodriguez, M. A.; Zechmann, C. A. <i>Inorg. Chem.</i> <b>2002</b> , 41, 2574-2582.
4	XEXSUP	2.247 Å	87.9 °	Piskunov, A. V.; Lado, A. V.; Fukin, G. K.; Baranov, E. V.; Abakumova, L. G.; Cherkasov, V. K.; Abakumov, G. A. <i>Heteroat. Chem.</i> <b>2006</b> , 17, 481-490.
4	NOWWAX	2.256 Å	90.3 °	Deacon, P. R.; Mahon, M. F.; Molloy, K. C.; Waterfield, P. C. <i>J. Chem. Soc., Dalton Trans.</i> <b>1997</b> , 3705-3712.
4	XEXSUP	2.273 Å	88.2 °	Piskunov, A. V.; Lado, A. V.; Fukin, G. K.; Baranov, E. V.; Abakumova, L. G.; Cherkasov, V. K.; Abakumov, G. A. <i>Heteroat. Chem.</i> <b>2006</b> , 17, 481-490.

4	CIXSUY	2.279 Å	87.1 °	Ramaswamy, P.; Datta, A.; Natarajan, S. <i>Eur. J. Inorg. Chem.</i> <b>2008</b> , 1376-1385.
4	TINOXL	2.311 Å	86.9 °	Christie, A. D.; Howie, R.A.; Moser, W. <i>Inorg. Chim. Acta</i> <b>1979</b> , 36, L447-L448.
	<b>Average:</b>	<b>2.233 Å</b>	<b>90.7 °/15 structures</b>	

<i>N</i>	CSD code	$d_{\text{Sn-O}}$	Reference
5	KAKBEF	2.380 Å	Zabula, A. V.; Filatov, A. S.; Petrukhina, M. A. <i>J. Cluster Sci.</i> <b>2010</b> , 21, 361-370.
5	KAKBEF	2.380 Å	Zabula, A. V.; Filatov, A. S.; Petrukhina, M. A. <i>J. Cluster Sci.</i> <b>2010</b> , 21, 361-370.
5	KAKBEF	2.383 Å	Zabula, A. V.; Filatov, A. S.; Petrukhina, M. A. <i>J. Cluster Sci.</i> <b>2010</b> , 21, 361-370.
5	KAKBEF	2.383 Å	Zabula, A. V.; Filatov, A. S.; Petrukhina, M. A. <i>J. Cluster Sci.</i> <b>2010</b> , 21, 361-370.
5	OFACSO	2.392 Å	Birchall, T.; Johnson, J. P. <i>J. Chem. Soc., Dalton Trans.</i> <b>1981</b> , 69-73.
	<b>Average:</b>	<b>2.384 Å/5 structures</b>	

<i>N</i>	CSD code	$d_{\text{Sn-O}}$	Reference
6	CIXTIN	2.394 Å	Ramaswamy, P.; Datta, A.; Natarajan, S. <i>Eur. J. Inorg. Chem.</i> <b>2008</b> , 1376-1385.
6	SIHQEF	2.415 Å	Ayyappan, S.; Cheetham, A. K.; Natarajan, S.; Rao, C. N. R. <i>Chem. Mater.</i> <b>1998</b> , 10, 3746-3755.
6	XEXSAU	2.423 Å	Natarajan, S.; Vaidhyanathan, R.; Rao, C. N. R.; Ayyappan, S.; Cheetham, A. K. <i>Chem. Mater.</i> <b>1999</b> , 11, 1633-1639.
6	XEXRUN	2.424 Å	Natarajan, S.; Vaidhyanathan, R.; Rao, C. N. R.; Ayyappan, S.; Cheetham, A. K. <i>Chem. Mater.</i> <b>1999</b> , 11, 1633-1639.
6	NTBZSN10	2.441 Å	Ewings, P. F. R.; Harrison, P. G.; Morris, A.; King, T. J. <i>J. Chem. Soc., Dalton Trans.</i> , <b>1976</b> , 1602-1608.
6	FOTDEX	2.481 Å	Holt, E. M.; Klaui, W.; Zuckerman, J. J. <i>J. Organomet. Chem.</i> <b>1987</b> , 335, 29-42.
6	HATCIQ	2.498 Å	Macdonald, C. L. B.; Bandyopadhyay, R.; Cooper, B. F. T.; Friedl, W. W.; Rossini, A. J.; Schurko, R. W.; Eichhorn, S. H.; Herber, R. H. <i>J. Am. Chem. Soc.</i> <b>2012</b> , 134, 4332-4345.
6	HATCOW	2.523 Å	Macdonald, C. L. B.; Bandyopadhyay, R.; Cooper, B. F. T.; Friedl, W. W.; Rossini, A. J.; Schurko, R. W.; Eichhorn, S. H.; Herber, R. H. <i>J. Am. Chem. Soc.</i> <b>2012</b> , 134, 4332-4345.
	<b>Average:</b>	<b>2.450 Å/8 structures</b>	

<i>N</i>	CSD code	$d_{\text{Sn-O}}$	Reference
8	VUTHUO	2.597 Å	Bandyopadhyay, R.; Cooper, B. F. T.; Rossini, A. J.; Schurko, R. W.; Macdonald, C. L. B. <i>J. Organomet. Chem.</i> <b>2010</b> , 695, 1012-1018.
<b>Average:</b>		<b>2.597 Å/1 structure</b>	

**Table S3.** Raman spectroscopic parameters of alkaline solutions containing Sn(II). The spectrum of the background solution has been subtracted.

$C_{\text{Sn(II)}}$ (M)	$C_{\text{NaOH}}$ (M)	Band at $\sim 430 \text{ cm}^{-1}$			Band at $\sim 490 \text{ cm}^{-1}$		
		$\sigma^a$ ( $\text{cm}^{-1}$ )	FWHM <sup>b</sup> ( $\text{cm}^{-1}$ )	I <sup>c</sup> (a.u.)	$\sigma^a$ ( $\text{cm}^{-1}$ )	FWHM <sup>b</sup> ( $\text{cm}^{-1}$ )	I <sup>c</sup> (a.u.)
0.10	4.0	434.9	55	0.81	486.2	35	0.30
0.15	4.0	433.4	61	1.44	491.1	50	0.83
0.20	4.0	433.4	56	1.67	487.7	43	0.64
0.25	4.0	433.7	62	2.40	489.8	45	1.08
0.10	8.0	438.7	69	0.80	496.7	53	0.68
0.15	8.0	440.5	69	1.72	495.3	35	0.42
0.25	8.0	437.6	54	1.99	492.6	58	1.36
0.10	4.0 <sup>d</sup>	430.6	70	1.00	490.2	52	0.63
0.20	4.0 <sup>d</sup>	432.9	68	1.81	489.9	53	1.02
0.10	$\sim 14^d$	448	66	1.17	505	48	0.65

<sup>a</sup> Raman shift

<sup>b</sup> Full bandwidth at half height

<sup>c</sup> Peak intensity

<sup>d</sup> KOH instead of NaOH

**Table S4.** Mössbauer parameters obtained for quick frozen aqueous alkaline solutions containing Sn(II). Measurements were performed at 78 K.

$C_{\text{Sn(II)}}$ (M)	$C_{\text{NaOH}}$ (M)	IS (mm/s)	QS (mm/s)
0.01	0.1	2.711	2.008
0.1	1.0	2.696	2.028
0.1	4.0	2.691	2.009
0.2	4.0	2.696	1.996
0.2	4.0	2.580	1.870
0.2	12.0	2.664	2.015
0.5	8.0	2.718	1.825

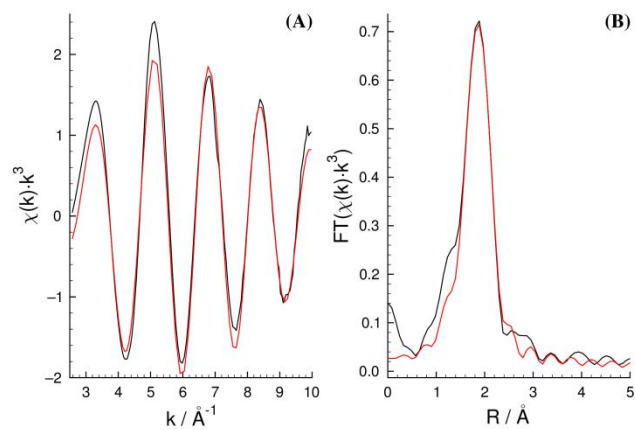


**Figure S1.** The experimental EXAFS spectrum of the Sn K-edge X-ray absorption spectra of  $0.1 \text{ mol} \cdot \text{dm}^{-3} \text{ SnCl}_2$  in  $1 \text{ mol} \cdot \text{dm}^{-3}$  hydrochloric acid (black) and the fitted spectrum (red) (A) and the Fourier-transform of the  $k^3$ -weighted EXAFS data of it and the fitted data (B).

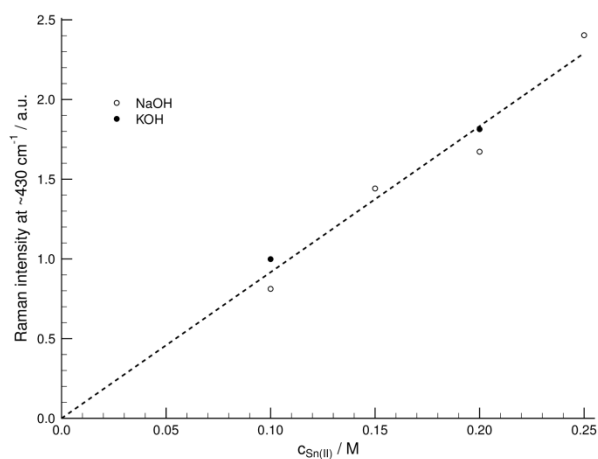


**Figure S2.** Integrated Raman band intensities for the mode at  $\sim 430 \text{ cm}^{-1}$ , after background subtraction and deconvolution, as a function of the  $C_{\text{Sn(II)}}$ .